Acta Geod Geophys (2014) 49:415–429
DOI 10.1007/s40328-014-0072-6

The role of geomechanical-based structural restoration in reservoir analysis of deepwater Niger Delta, Nigeria

E. K. Nyantakyi · Li Tao · Hu Wangshui · J. K. Borkloe

Received: 11 June 2014 / Accepted: 30 September 2014 / Published online: 18 October 2014

Abstract Recent advancements in fields of geomechanics and structural geology have given rise to geomechanical-based structural restoration method. This study investigated the role geomechanical-based structural restoration in reservoir analysis for Boko discovery in the proximal part of the outer fold thrust belt, deepwater Niger Delta, Nigeria. Results of the study revealed the significance of the geomechanical-based structural restoration method in validating interpretation, re-constructing structural history, and gathering insight into the deformation mechanisms and rock property evolution. The main advantage of this method over the more conventional methods is that the conventional method is not imposed as an input. In addition, several quantitative deformation parameters can be output to enable us understand the structural genesis and potential effect on petroleum system. Finally, quantitative estimates of deformation and stress may be used to respond to challenging questions related to trap history, evolution of reservoir and seal, and permeability heterogeneity within reservoirs in the near future.

Keywords Geomechanical-based restoration method · Deformation mechanism · Flexible boundary conditions · Structural analysis · Deep water · Niger Delta · Nigeria

1 Introduction

The petroleum industry has taken early steps towards exploiting large resources available in complex and often unconventional oil and gas plays around the world within the last decade. Typical example is the shale gas plays in the US and around the world's production from which depends on the interconnectivity of existing and induced fractures formed under distinctive stress regimes.

E. K. Nyantakyi · L. Tao · H. Wangshui · J. K. Borkloe
School of Earth Sciences, Yangtze University, Caidian, Wuhan 430100, Hubei, China

E. K. Nyantakyi (✉) · J. K. Borkloe
Civil Engineering Department, Kumasi Polytechnic, P.O. Box 854, Kumasi 03220, Ghana
e-mail: emmanuelkwesinyantakyi@yahoo.com

Basin analysis has advanced in recent years to answer the distinctive questions arising from the above. Basin modeling work flow involves capturing evolution of the structural kinematics by starting with the present day subsurface geometry. The process involves the use of various methods that range in complexities from a simple back-stripping of layered strata to 3D geomechanics based structural restoration. Geomechanics based structural analysis utilizes realistic boundary conditions applied on rocks having distinctive mechanical properties that simulate natural deformation processes (Maerten and Maerten 2006). The basic "rule" of this process is based on the principles of conservation of mass, momentum, and energy that is common in all aspects of solid mechanics. Other hybrid techniques also in vogue (Guzofski et al. 2009; Plesch et al. 2007; Durand-Riard et al. 2011) have been used in analysis and are based on global minimization of strain.

There are several advantages of using geomechanics-based structural restoration method as inputs to basin modeling. Firstly, horizontal component of deformation can be critical in compressional or strike-slip structural settings and also in proximity of deforming salt bodies as stress anisotropy is generally coincidental with fluid-flow or permeability anisotropy directions. Most basin modeling platforms do not effectively capture this aspect of deformation, as within most basin model applications particles move in a vertical direction during deformation. Therefore the incorporation of geomechanical restoration method can help refine basin models. Secondly, geomechanics-based restoration method can predict the tendency for faults to dilate and slip during specific time periods of structural growth. These discrete fault zones may act as conduits for hydrocarbon migration pathways or entrapment surfaces. Such observations can help constrain hydrocarbon migration episodes during critical time steps. Finally, geomechanical models can output deformation attributes that can help diverse subject areas including identification of structural style, fracture prediction, rock property prediction or overall trap integrity. The geomechanics-based restoration method was used to test the validity of structural interpretation; to explicit strain determinations that are product of restorations to aid structural analyses, and to gain insight into deformation process without the imposition of a kinematic model. Figure 1 shows the map of major structural provinces of offshore Nigeria including both deep-water and shelf.

The sedimentary section in deep-water Niger Delta provided excellent opportunities to study evolution of a variety of structural styles in passive margin settings (Doust and Omatsola 1990). The structural framework was provided by depth-converted 3D seismic data and consists of deformed Mesozoic/Paleocene through Recent clastic strata. The structural trend evolved primarily during the Miocene. Structures form above a mobile detachment. In deep-water Nigeria, the detachment consists of a thick, overpressured, Paleocene shale unit called the Akata Formation (also the primary source interval). Cross-section A-A' (Fig. 2) is a regional seismic transect through the study area clearly showing the extension zone as having several major normal faults, followed by a belt of intensely deformed inner fold thrust structures that transition into the outer fold-thrust belt.

The transitional zone between the inner and the outer fold-thrust belt is a prolific petroleum province having large discoveries, such as Agbami, Akpo, Nnwa-Doro, Bolia-chota, and others. The primary structural style in these discoveries is detachment folding having inflated cores of the Eocene overpressured Akata shale. There are several notable discoveries in the inner fold-thrust belt that include Bonga, Aparo and Uge. In contrast, the exploration results in outer fold-thrust belt structures in deep-water Nigeria, which more closely resemble shear fault bend style folds, have been noted generally to lack significant hydrocarbon accumulations.

Availability of high quality seismic data especially in the outer fold-thrust belt helps in constraining the kinematics of structural growth. Analog well data are used to characterize

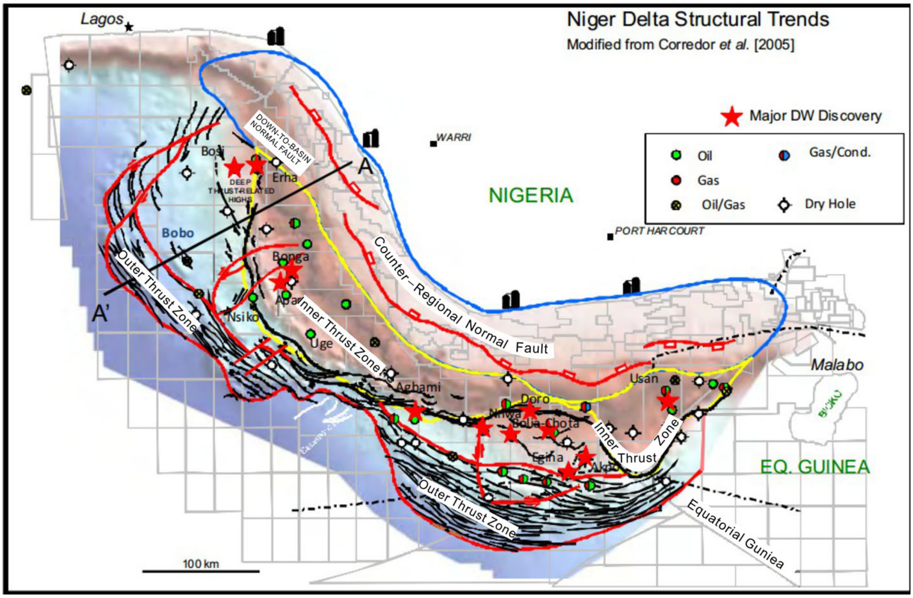

Fig. 1 Regional structural provinces in the Niger Delta basin showing structural provinces and associated faulting patterns. Shades of *blue* represent the deep water parts of the basin. Major discoveries are indicated. AA' shows the location of the regional transect described in text. (Color figure online)

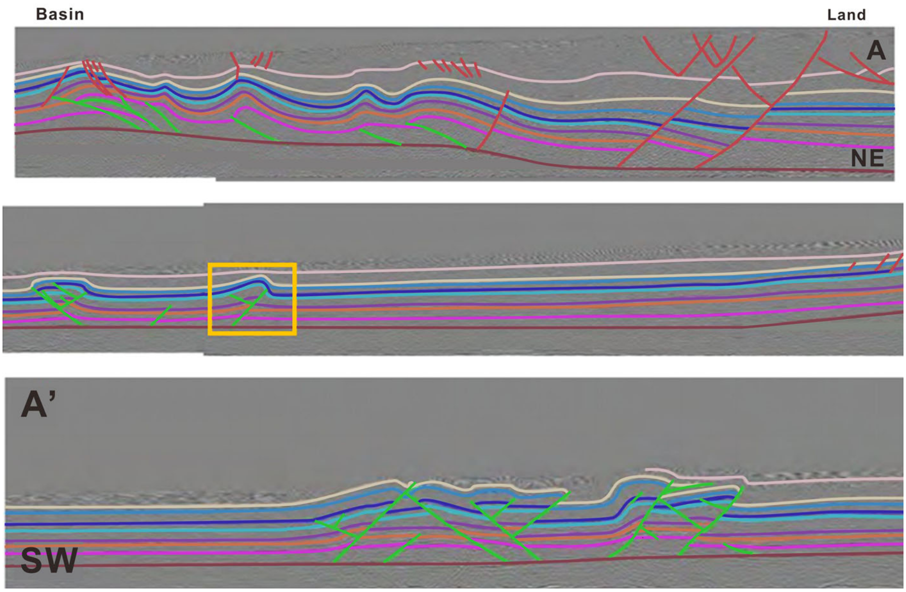

Fig. 2 Regional seismic transect through the Niger Delta from shelf to deep-water showing the various structural provinces shown in Fig. 1. North-east–south-west there is a progression from zones of extension and associated normal faulting to an earlier fold-thrust belt, a quiet zone, an outer folded thrust belt, and the abyssal plane. The *gold colored box* is the study area around the Bobo discovery. Note that vertical axes are in Two-Way-Travel Time (ms). Seismic courtesy ION Geophysical. (Color figure online)

the elastic geomechanical properties such as Young's modulus, Poisson's ratio, cohesion, and friction angle as well as density and compaction coefficients for individual stratigraphic units. The above present day material properties evolve during stages of restoration. Geomechanics-based restoration method uses principles of conservation of mass, momentum, and energy during retro-deformation of geologic structures. This is in contrast to balancing line length, area, or volume that forms the framework of kinematic restorations. In addition, kinematic restorations often require a pre-determined kinematic development of structural history to be assumed and tested during restoration.

2 Methodology

Three different methods were employed in investigating the structural analysis of deepwater Niger Delta and these were described as follows.

2.1 Geomechanics-based restoration

The specific structure selected for the study is the Bobo discovery (Kostenko et al. 2008) in the proximal part of the outer fold thrust belt. Availability of well data provided local stratigraphic age control and lithologic information. A series of Paleocene through recent strata were mapped in the seismic data. This structural complex was well-imaged and comprised of two east dipping fold-thrusts and an associated west-dipping back-thrust. The thrust verged to the west in the south and was characterized by a long back limb and a short forelimb. This is a commonly observed geometric characteristic in the deep-water Niger Delta and was described as shear fault bend fold (Corredor et al. 2005). It was suggested that the thick and ductile upper Eocene Akata Shale interval resulted in an inclined shear profile in the lower section of the fold as opposed to the vertical profile in fault-bend fold (Suppe 1985) style more commonly observed in indurated and brittle rocks. The detachment was in the upper Eocene throughout most of the structure and climbed up section slightly to the north. The growth of the structure appeared to be upper middle Miocene through the present. At location L2, the vergence remained towards the west, though the crestal part of the structure gained complexity and could be interpreted to be due to the additional deformation associated with a shallower detachment in the middle Miocene. At both locations L2 and L3, the folding in the crest was pronounced. At the L3 and L4 locations, the vergence changed to the east as the thrust lost throw which was presumably picked up by the back thrust. At location L4 through location L7, the geometry assumed more of a box-fold shape because of the presence of both the thrust and the back-thrust. Finally, deformation terminated and structural relief was lost around location L8 where the structure verged to the west as in the south.

2.2 Material property characterization

Conventional restorations are driven by the geometry of the deformed state and assumed kinematics of deformations together with assumptions on geometric conservation (line length or area typically) as a proxy for rock mass conservation. In general, this assumed brittle, rigid body translation or rotation, and negligible internal distortion. There was no dependence on mechanical properties of the sequence of rocks that together comprised the mechanical stratigraphy. In contrast, the resultant stress during any geomechanics-based restoration step was a function of the deformed state geometry, restoration boundary condition, and also mechanical properties of the deformed rocks such as Young's modulus and Poisson's ratio. In the current implementation, the restoration assumed a linear elastic constitutive relationship that ensured complete reversibility between deformed and restored stages. Linear elasticity had a simple assumption that was violated by deformation of porous tertiary rocks especially when considering deformed structures that had undergone large strain. However, linear elastic behavior most closely approximated conventional kinematic restoration and provided a basis for comparison.

2.3 Boundary conditions for restoration

Dynel 2D used in this study uses linear elasticity as the constitutive relation and implements a finite-element solver using appropriate imposed boundary conditions. In addition to the paleo-structural configuration at each pre-determined time step, various stress and strain related properties are obtained and can be used to constrain sub-seismic deformation, fault reactivation, and other petroleum system related issues.

One of the critical steps in any geomechanics-based restoration analysis is the imposition of appropriate boundary conditions. Conventional kinematic analysis or basin modeling applications are based on back-stripping analysis or simply flattening vertical shear where respective chrono-stratigraphic unit is flattened to a preset datum, often horizontal, or an assumed depositional slope. This type of boundary condition may be somewhat suited for several types of structures including those formed due to gravitational collapse but is less suited for restoration of thrust, transpressional or purely strike-slip structures.

Unfortunately, current implementation of Dynel 2D was limited to restoration of a structural top to a datum rather than imposing displacement on the boundary walls or sides of the structure to effectively pull back thrust or strike-slip structures. However, the results served as a basis for evaluation of the technique in comparison to conventional kinematic restoration techniques. Boundary conditions used in the restorations included (i) flattening the restoration surface to a preset flat datum elevation. Horizontal paleo-bathymetry is a reasonable assumption for relatively short ($\sim$9–12 Km) section lines from middle Miocene to present day; (ii) the mapped basal detachment was allowed to slip in the horizontal direction either in the foreland or the hinterland direction depending on the direction of the dip of the fault (e.g., hanging wall in sections L1 and L8 were allowed to slide back towards the hinterland while the detachment was locked from moving towards the foreland), all other sections were allowed to slide along the thrust and back-thrust in both directions; (iii) the sub-detachment vertical wall on eastern side of the structure was locked from moving in the vertical or horizontal direction. This allowed the hanging wall and footwall blocks along the ramp sections of the fault to slide past one another.

3 Results and discussions

3.1 Geomechanics-based restoration method

Geomechanics-based restoration were conducted on eight lines (L1–L8) shown in Fig. 3 using the boundary conditions outlined above. At every restoration step, stress and strain properties (including magnitude and trajectories of the two principal stress/strain; vertical, horizontal, and shear stress/strain) along with slip-offset was generated at each nodal point within the model.

Figure 4 shows the seismic cross-sections L1–L8 illustrating the variation in structural style from the south-east to the north-west. Eight different northeast-southwest trending depth

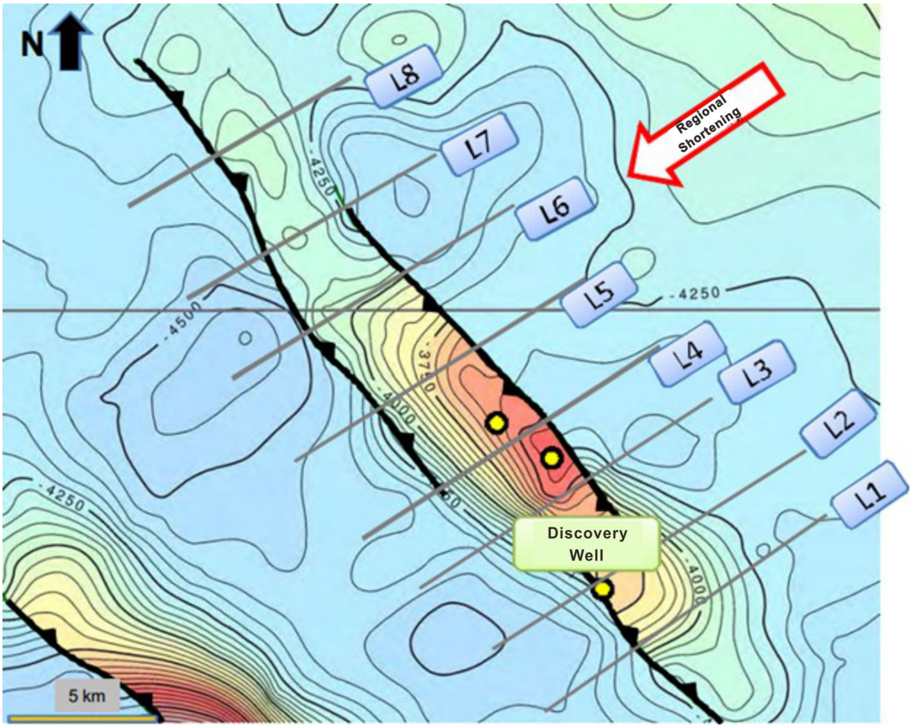

Fig. 3 Depth structure map of middle Miocene showing line of sections L1–L8 from southeast to northwest. Note the northwest–southeast trending thrust faults. Contour labels are subsea depths in meters. Contour interval is 50 m.

cross-sections (L1–L8) were restored using Dynel 2D. For each geological unit, average log derived mechanical properties (Young's modulus and Poisson's ratio) and rock mass properties (bulk density, porosity, and compaction coefficient) were input (Figs. 5, 6, 7). Each cross-section was restored to a specific horizontal datum, decompacted, and restored through five time steps in Pliocene—middle Miocene. Results from sequential restoration for a single line at top Pliocene and upper middle Miocene time-step is shown in the following section (Fig. 8a, b). The nature of the results from L1 in Pliocene stage and middle Miocene stage has been illustrated in Fig. 8a and b, respectively.

In Fig. 8a, the Pliocene sequence boundary has been flattened or unfolded to a horizontal datum. Negligible horizontal strain that can be attributed to unfolding only is observed in the restored state. Even though the fault and detachment is free to slide back towards the hinterland (west) no apparent slip is observed; western vertical boundary of hanging wall shows no offset from section below detachment. This is corroborated by looking at growth pattern in the present day cross-section (Fig. 4, L1) that shows slight thinning at the crest. The rest of the structure including the footwall is generally undeformed (absence of horizontal strain contours). The above characteristics is in marked contrast in the middle Miocene restored stage (Fig. 8b). Significant amount of slip appears to be recovered in restored state along most layers below the restored middle Miocene surface. This is also evidenced by appreciable displacement of the hanging wall vertical boundary relative to the section below the detachment. Large horizontal strain gradients are seen restricted to the hanging wall while

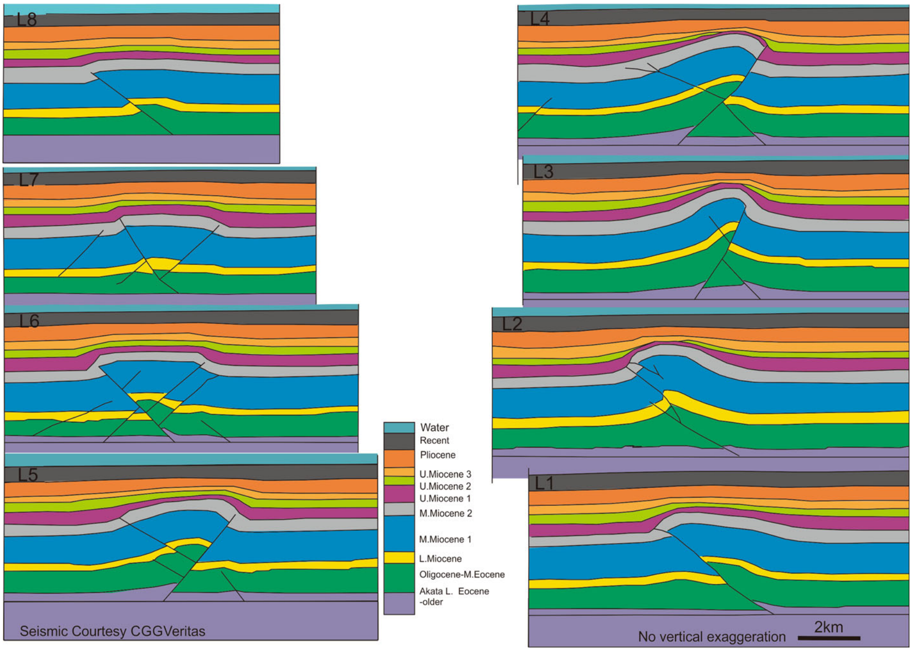

Fig. 4 Seismic cross-sections L1–L8 as shown on inset map across the structure illustrating the variation in structural style from the south-east to the north-west. Refer to text for detailed description

the footwall is relatively undeformed. Note the concentration of contours at the fault tip that is caused by stratal rotation setting up large horizontal strain gradients that is largely a result of the flattening boundary condition that is imposed. There is a strain concentration along the base of the ramp section highlighting the potential for large strains in the region of transition from flat to a ramp.

In summary, the restoration suggests that the interpretation is largely valid, as almost all fault slip is recovered and no large thickness mismatches are apparent.

An outcome of the process of any restoration technique whether kinematics or geomechanics based as shown here lies in confirming the validity of the interpretation or iteratively making the structural interpretation more permissible. Once the interpretation is tested to be valid, the results can further illuminate structural evolution.

3.2 Material property characterization

The stratigraphic column in deep-water tertiary sediments was dominated by mud-rocks with minor proportion of coarse-grained clastic rocks. The overall net to gross of major third order sequences in deep-water tertiary turbidites was approximately on the order of 10 %, the mechanical properties of clean shale was used to represent the simplified mechanical stratigraphic column. Young's modulus and Poisson's ratio were calculated using standard relationships between these properties and dynamic measurements in the well such as P- and S-wave velocity and density computed from sonic and bulk density logs. In addition, two more geomechanical strength parameters cohesion (cohesive shear strength) and friction angle were also determined from well log measurements.

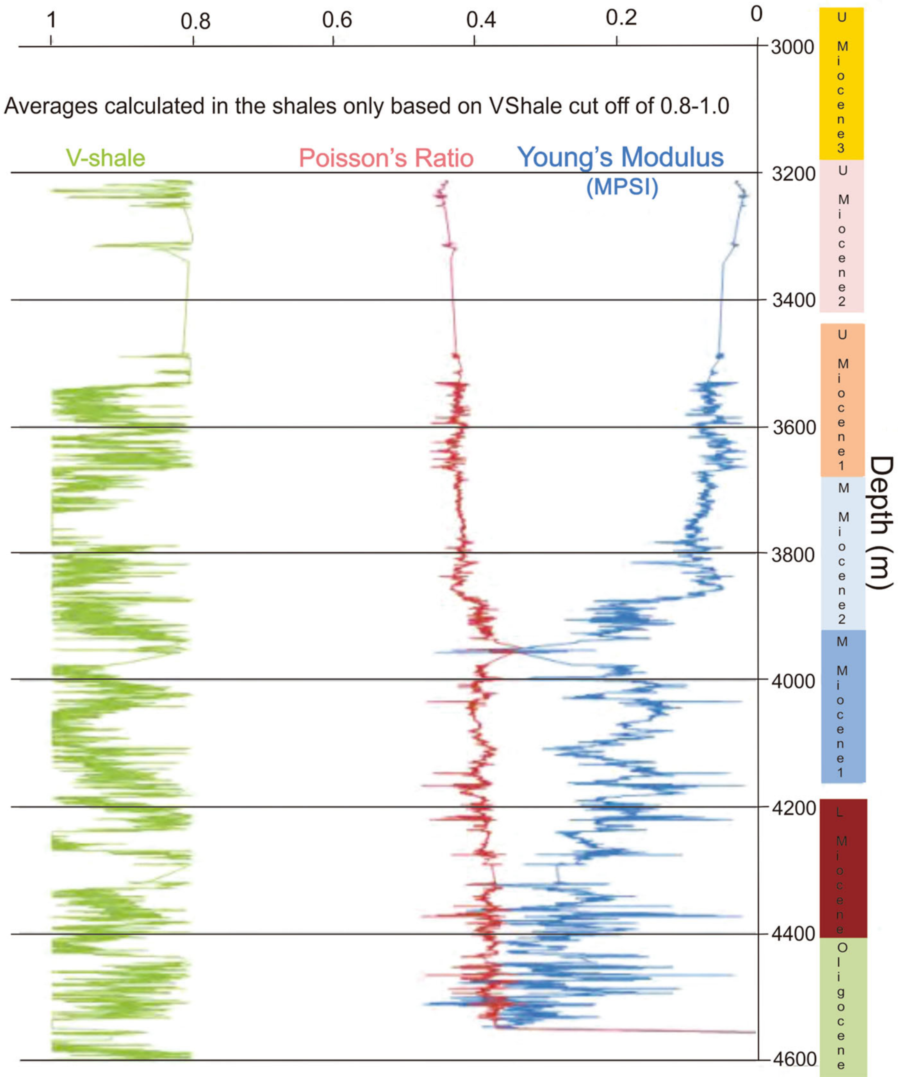

Fig. 5 Mechanical property characterization based on example well data. Averages over third-order sequences are calculated in clean shale only using a Vshale value of 0.8–1.0. Note that vertical scale is in depth (m) and the scale for "Young's Modulus" is between 0.2 and 0.4

Three wells were used in the deep-water part of the Niger Delta Basin and separated by a total difference of about 200 km. These wells had log suites that ensured high quality of the determined mechanical properties. Property determinations were made every 0.15 m and then data averaged over major third-order sequence boundaries. Figure 6a shows the evolution of Young's modulus as a function of depth below mud line (and age of sediments). Young's modulus increases to a depth of 2,400 m below mud line (DBML) before decreasing. This depth of reversal was related to the onset of abnormal pressure in the sedimentary section that resulted in under-compaction relative to the shallower normally pressured section. Other

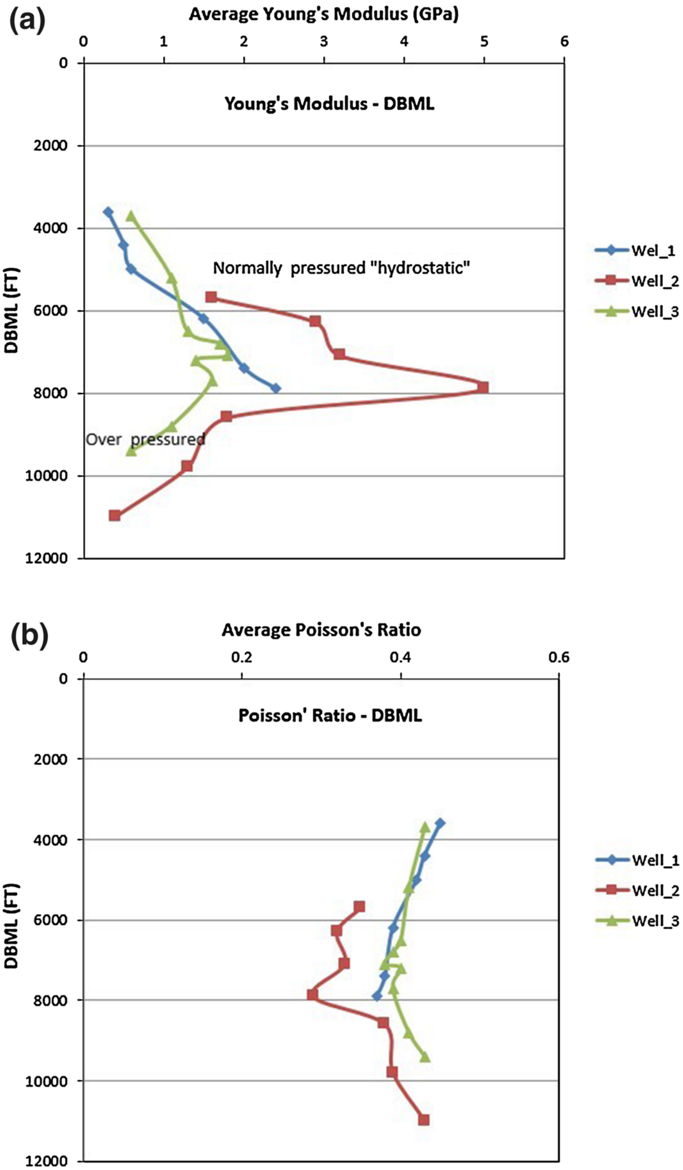

Fig. 6 Variation of average mechanical property **c** cohesion, and **d** Friction angle; depth is below mud line (DBML). Note the increasing trend in Young's modulus **(a)** and cohesion and decreasing Poisson's ratio **(b)** with depth below mud line in the shallow normal (hydrostatic) pressured section and contrast with over-pressured sections at a greater depth. The depth at which this reversal occurs is often the onset of abnormal pressure in tertiary basins

properties also showed a similar behavior. Poisson's ratio (Fig. 6b) decreased to a value of 0.35 before starting to increase again at the depth corresponding to onset of overpressure. Cohesion increased in the normally pressured section before decreasing at the onset of over-pressure (Fig. 6c). Friction angle showed a slight but consistent decrease as a function of DBML or geologic age. In the abnormal pressure section, rocks behaved in a manner similar

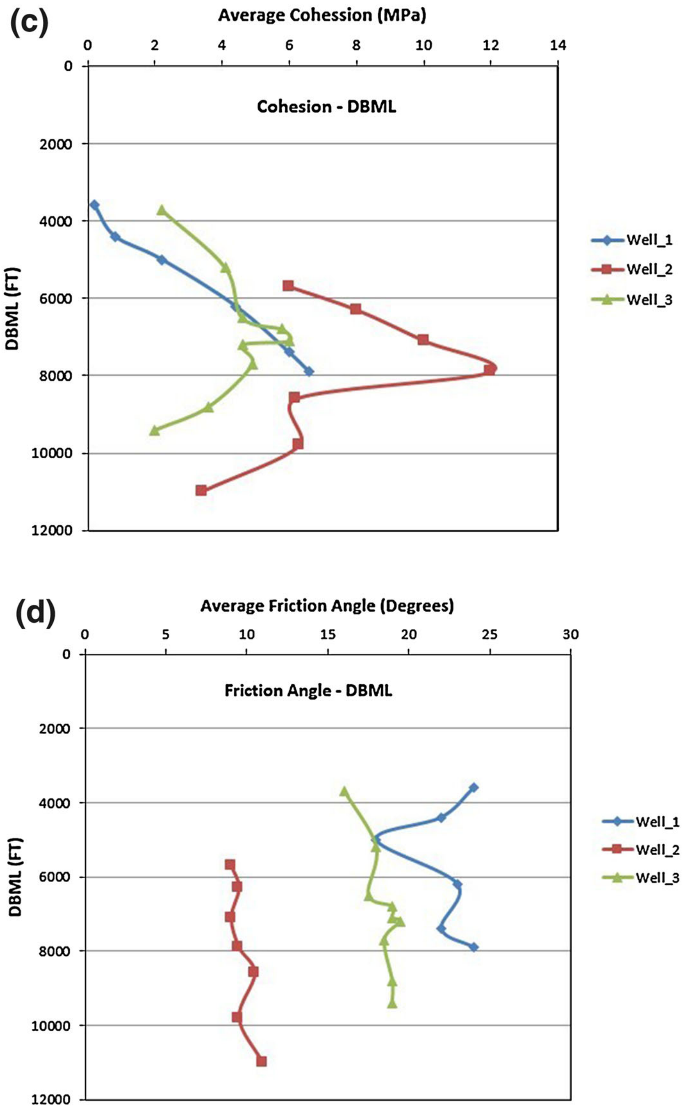

Fig. 6 continued

to shallower burial as pore space remained open due to lack of expulsion of the pore water. One of the primary deformation mechanisms of young tertiary sedimentary rocks is through the process of compaction that resulted in progressive loss of porosity as a function of increasing burial depth (DBML). The effect of compaction and consequent porosity loss resulted in the evolution of most conceivable mechanical properties such as increased bulk density, higher velocity sediments. A key part of the process of restoration is the associated simultaneous decompaction that resulted in increased porosity due to the process of back-stripping and a resultant inflation or thickening of younger strata progressively towards depositional thickness. As it has been shown that porosity evolution is exponential with burial depth (Athy

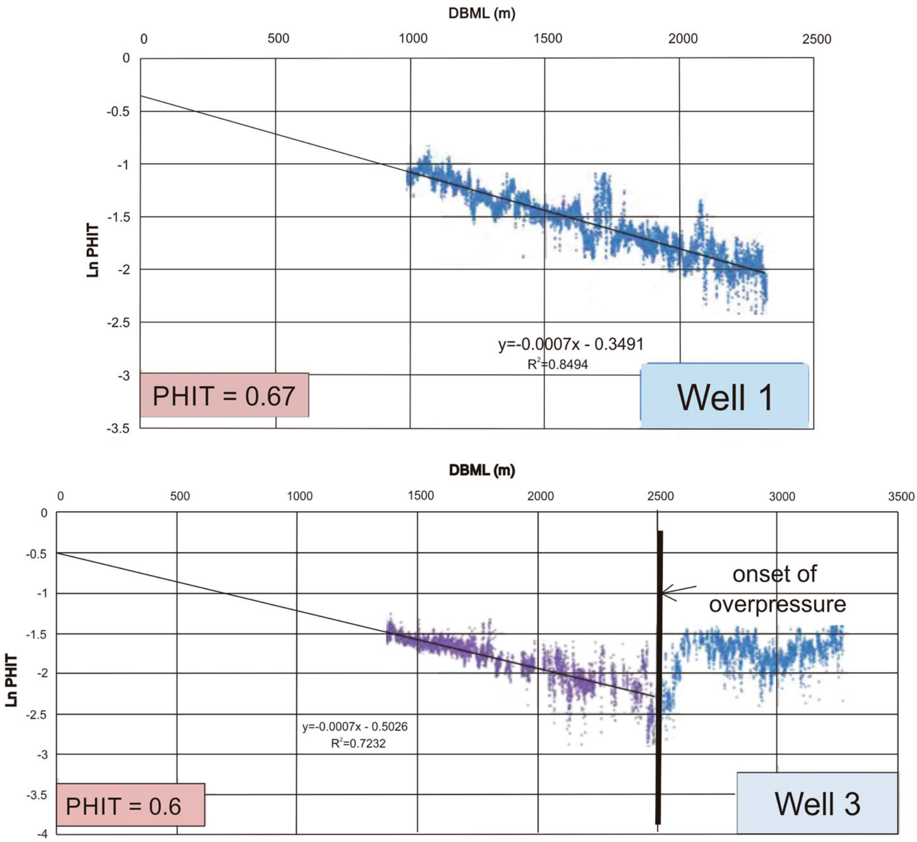

Fig. 7 Compaction co-efficient or slope of the best-fit line derived from the total porosity log data from two wells in deep-water Niger delta. The projected intercept defines the depositional porosity (at the mud line)

1930), the "rate of compaction" or compaction co-efficient is characterized by the slope of the natural logarithm of total porosity as a function of burial depth. Figure 7 showed the results from two of the previously described wells suggest that compaction follows a very similar trend in various parts of the deepwater Niger Delta. This is evident from a remarkable similarity in the compaction co-efficient or slope of the best-fit line. The intercept of the straight line determined by linear regression on the porosity axis represented the depositional porosity. In the plots shown (Fig. 7) this value was observed to fall in the reasonable range of 60–67%.

It was argued that because of the incorporation of measured (logged) rock properties and resultant finite strain computations, these results can be valuable. An extended analysis to sections through L8 shows a rate of shortening plot, Fig. 9 across sections. In all sections except for sections L2 and L3, the rate of shortening reaches maximum in the time span of 9–13 Ma. In sections L2 and L3, the shortening rate reaches a maximum at around 7 Ma. This raises a genetic question on the specific mechanism and sequence of development of the entire structural complex. In Fig. 10, maximum relief is plotted along with net fault slip and longitudinal strain as a function of the distance along the trend. The structural relief reaches a maximum along cross-section L3, but neither the fault slip (maximum along L6) nor the longitudinal strain is at their maximum at this location.

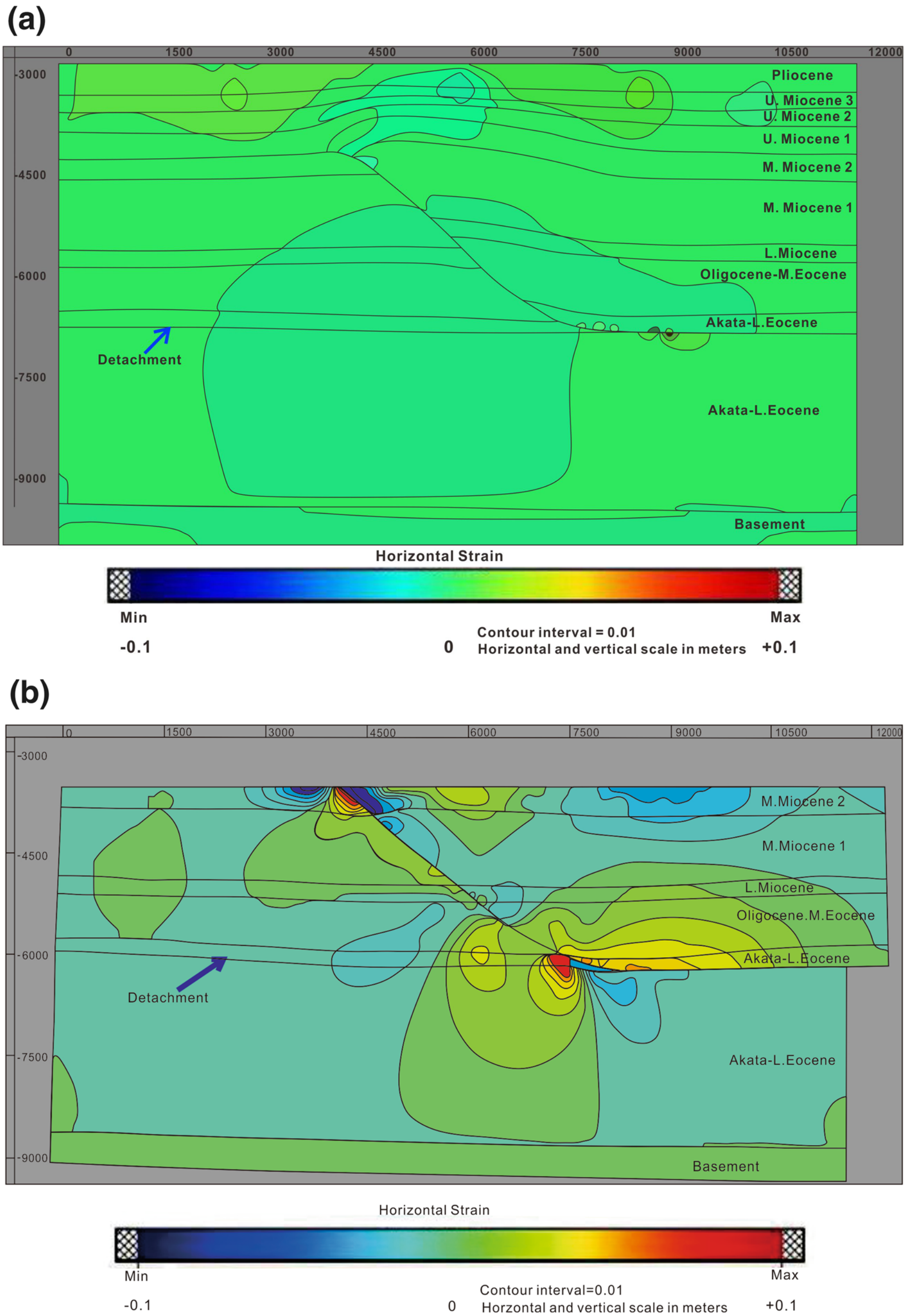

Fig. 8 **a** Geomechanical restoration of L1 at top Pliocene, with horizontal strain overlay showing strain concentration on the structural crest and fault branch point area. *Color bar* represents maximum positive and negative strains of 10 **b** Geomechanical restoration of L1 at top middle Miocene, with horizontal strain overlay showing strain concentration on the structural crest and fault branch point area. Note the general flattening of the horizon and transfer of slip due to restoration towards the hinterland suggesting a valid interpretation

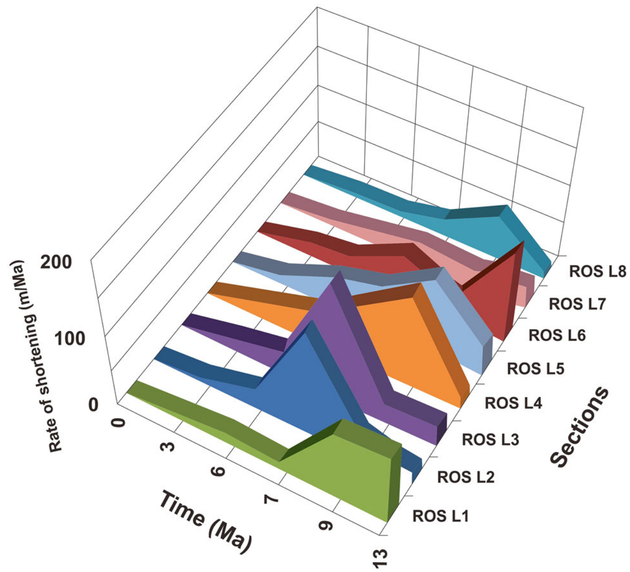

Fig. 9 Deformation history through the structure showing temporal and spatial along trend variation of rate of shortening. Note the activation of different thrusts and deformation in the transfer zones. Earliest movement on forethrusts (L1), Back-thrust activated from the north (L4–L5), large movement on back-thrust during 6–8 Ma (L2 –L3)

These observations are difficult to explain by a single known deformation mechanism. If the structures were formed by fault bend type folding mechanism the fault slip maxima would be coincidental with the structural relief maxima or the longitudinal strain maxima. The difference between strain and slip maxima locations suggest a degree of disharmonic folding in addition to fault related folding. Highest structural relief occurs spatially removed from strain and fault slip maxima, possibly suggesting detachment folding. As mentioned before detachment folding is a common structural style in the zone between the inner and outer fold-thrust belts including at several large discoveries. In the restoration example shown here, geomechanical-based restoration is driven by (i) boundary conditions, (ii) constitutive relationship, and (iii) the mechanical properties of the rock column. Current implementation of the restoration algorithm as presented is limited by the inability to impose the most appropriate boundary condition. Use of elasticity while appropriate for comparing results with conventional kinematic methods is inappropriate for analysis of isolated structural complexes especially in young, tertiary sediments that have significant porosity changes and plastic strain accumulation during deformation.

3.3 Boundary conditions for restoration

A combination of inappropriate boundary condition and constitutive relationship may result in inconsistent displacements and resultant strain values. Therefore, stress calculations are suspect as it is a simple linear transform using determined strain values and elastic constants. However, a more sophisticated implementation that improves boundary condition flexibility and removes limitation imposed by reversibility of deformation pathway (relaxes use of linear elasticity) may allow investigation of the entire dynamics (including stress magnitudes) and genesis of structural complexes.

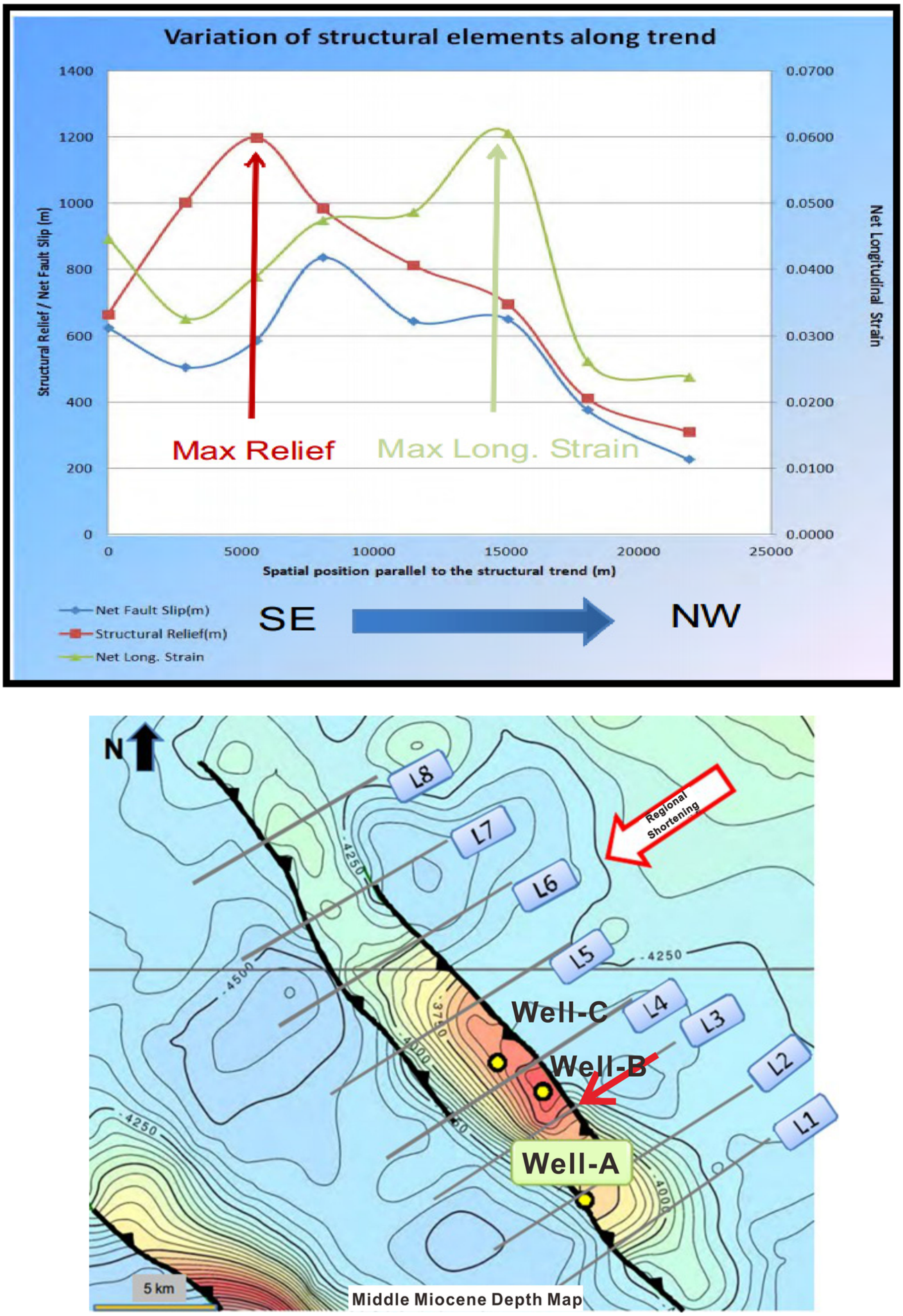

Fig. 10 Variation of structural relief, net fault slip, and net longitudinal strain along the length of the structure. Refer to text for explanation

Constraints on aspects of basin analysis can include span of critically stressed time window of key faults, suggesting timing of hydrocarbon migration relative to structure formation (charge) or trap breach due to fault reactivation (trap integrity or leakage); zones of enhanced permeability and/or permeability anisotropy related to fracture/fault intensity and its impact on reservoir flow heterogeneity; better understanding of compaction especially in areas of salt/shale diapirs where the stress tensor is rotated and impacts mean effective stress thought to control reservoir compaction.

4 Conclusions

A 2D geomechanical-based restoration method was conducted on an isolated structural complex in deepwater Nigeria and the results showed important details on the genesis and evolution. The spatial separation along the structure between the points of maximum relief, maximum fault slip, and maximum longitudinal strain suggests the disharmonic nature of folding and a likely detachment folding style deformation during stages of structural development as opposed to a shear fault-bend fold style. The research also proves the viability of validating structural interpretation through a geomechanical-based restoration method as opposed to conventional kinematic restoration. The clear advantage of the technique is that no kinematic model is assumed or applied and restoration is achieved through application of basic principles of physics. Future progress in implementation of such restoration methods, use of more flexible boundary conditions, and appropriate constitutive relationships can result in improved constraints on critical basin analysis questions related to hydrocarbon migration, trap integrity, or leakage, reservoir compaction, and fluid-flow heterogeneity.

Acknowledgments The authors would like to acknowledge the management of Kumasi Polytechnic, Kumasi headed by the Rector Prof. N. N. N. Nsowah-Nuamah, for providing financial assistance to undertake this study. Special thanks to ION Geophysical and CGG-Veritas for permission to use the seismic images for this study.

References

Athy LF (1930) Density, porosity, and compaction of sedimentary rocks. AAPG Bull 14:1–14

Corredor F, Shaw JH, Bilotti F (2005) Structural styles in the deep-water fold and thrust belts of the Niger Delta. AAPG Bull 89:753–780

Doust H, Omatsola E (1990) Niger Delta in divergent/passive margin basins. In: Edwards JD, Santogrossi PA (eds) Divergent/passive margin basins. AAPG Memoir, Tulsa, pp 201–238

Durand-Riard P, Salles L, Ford M, Caumon G, Pellerin J (2011) Understanding the evolution of syndepositional folds: coupling decompaction and 3D sequential restoration. Mar Petrol Geol 28:1530–1539

Guzofski C, Müeller J, Shaw JH, Muron P, Medwedeff D, Bilotti F, Rivero C (2009) Insights into the mechanisms of fault-related folding provided by volumetric structural restorations using spatially varying mechanical constraints. AAPG Bull 93:479–502

Kostenko O, Naruk SJ, Hack W, Poupon M, Mayer H-J, Mora-Glukstad M, Anawai C, Mordi M (2008) Structural evaluation of column-height controls at a fold-thrust discovery, deep-water Niger Delta. AAPG Bull 92:1615–1638

Maerten L, Maerten F (2006) Chronologic modeling of faulted and fractured reservoirs using geomechanically based restoration: technique and industry applications. AAPG Bull 90:1201–1226

Plesch A, Shaw J, Kronman D (2007) Mechanics of low-relief detachment folding in the Bajiaochang field Sichuan basin, China. AAPG Bull 91:1559–1575

Suppe J (1985) Principles of structural geology. Prentice Hall, Englewood Cliffs, p 537